Journal of Research of the National Bureau of Standards Vol. 58, No. 1, January 1957 Research Paper 2728

Phase-Diagram Study of Alloys in the Iron-Chromium-Molybdenum-Nickel System

C. J. Bechtoldt and H. C. Vacher

Alloys in the iron-chromium-molybdenum-nickel system were examined after quenching from 2,200°, 2,000°, 1,800°, 1,650°, and 1,500° F. Compositional limits of stability of seven phases were summarized in diagrams. Fe_2Mo was found to be a stable phase; and a ternary phase, not previously reported, was identified to have the approximate composition of 4 percent of chromium, 53 percent of iron, and 43 percent of molybdenum.

1. Introduction

A study was made recently at the Bureau [1,2][1] of the microstructures in austenitic stainless steels containing approximately 3.5 percent of molybdenum. This study showed that the microconstituents sigma (σ), chi (χ), and carbides could be separated from the alpha iron (α Fe) and gamma iron (γ Fe) phases by dissolution and then identified by X-ray diffraction. The study also revealed a dearth of information in phase diagrams that would define the ranges of composition and temperature of stability of σ and χ in quaternary alloys of the iron-chromium-molybdenum-nickel system. Accordingly, an investigation was started with the purpose of supplying information of this kind.

The six binary systems involving chromium, iron, molybdenum, and nickel have been studied extensively, and apparently reliable phase diagrams are available over a wide range of temperature. However, the information on the four ternary systems was sufficiently complete to permit construction of diagrams only at 2,200° F. Obviously a comprehensive investigation of the entire quaternary system would require an immense amount of work. It was decided, consequently, that attention would be focused on iron-chromium-molybdenum-nickel alloys containing 70 percent of iron. The work then would be of interest in the field of heat-resisting alloys and at the same time furnish data to check contemporary isothermal phase diagrams of the chromium-iron-molybdenum, chromium-iron-nickel, iron-molybdenum-nickel, and iron-molybdenum systems.

2. Experimental Procedures

2.1. Plan of Investigation

Limiting the investigation to 70-percent-iron alloys made it possible to investigate the alloys at several temperatures, thus making it easier to compare the results with previous investigations. The α Fe and γ Fe phases have wide solubility ranges at 2,500° F, and the reactions that result in the formation of σ and χ are moderately fast at temperatures above 1,500° F. Thus equilibrium could be attained in a reasonable time, and the reactants could be quenched. The wide solubility ranges facilitated the preparation of the alloys from the powdered metals. Seventy-percent-iron alloys, made from chromium, iron, molybdenum, and nickel powders, whose source and purity are shown in table 1, were sintered at 2,500° F, cooled slowly to room temperature, reheated to 2,200°, 2,000°, 1,800°, 1,650°, and 1,500° F, and then quenched to room temperature. A large range of compositions was covered (fig. 1)

TABLE 1. *Manufacturer and chemical analyses of metal powders*

Metal powder	Manufacturer	Chemical analysis
		%
Molybdenum	Johnson, Mathey & Co.	99.9 minimum.
Do	Charles Hardy, Inc.	99.9 minimum.
Nickel	International Nickel Co., courtesy of Francis B. Foley.	[a] Spectrographic method: 0.01 Al, 0.001 Co, 0.001 Cu, 0.1 Fe, 0.001 Mg, 0.001 Mn, 0.001 Pb, 0.01 Si.
Do	Metal Disintegrating Co.	[a] Spectrographic method: 0.1 Al, 0.001 Ca, 0.01 Cr, 0.1 Cu, 0.01 Mg, 0.001 Pb, 0.01 Ti. Chemical methods: 0.12 Co, 0.09 Fe, 0.06 Si.
Chromium	Electro Metallurgical Co., courtesy of Russell Franks.	Chemical methods: 0.01 C, 0.03 Fe, 0.01 Cu, 0.01 Pb, 0.033 S, 0.54 O, 0.012 H, 0.008 N.
Iron	General Aniline & Film Co.	Carbonyl iron: 99.6 to 99.9.

[a] Values are maximum limits. Analyses of nickel were made at the Bureau; the others were given by the manufacturers.

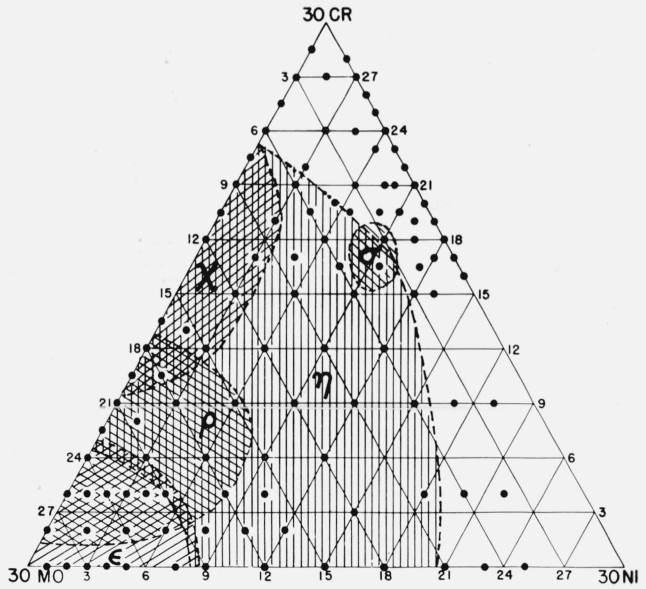

FIGURE 1. *Compositions of alloys investigated containing 70 percent of iron and areas in which hard phases were found after sintering treatment at 2,500° F and furnace cooling.*

[1] Figures in brackets indicate the literature references at the end of this paper.

so that the boundaries of phase stability could be bracketed by determining the identity of the phases present in the alloy. To do this, microscopic examination of etched surfaces was used to reveal how many phases were present, and a qualitative analysis of separated residues by X-ray diffraction was made to indicate what phases were present.

2.2. Preparation of Alloys

Thirty-gram mixtures of the powdered metals were made to predetermined compositions. The mixing was done in a machine similar in design to that used for mixing amalgams in dental laboratories. The mixing jar was fastened to an arm attached to a bearing whose shaft was both off-center and slanted relative to the 1,750-rpm motor on which it was mounted, as shown in figure 2. The opposite end of the arm was held by a spring. After mixing the charge, 2-g pellets, ½ in. in diameter, and 3/32 in. thick, were made by using 60,000-lb/in.^{2} pressure in the compacting operation.

The chromium content was determined by chemical analysis in several pellets of a number of alloys in order to check the uniformity of mixing. Comparison of chromium content in duplicate pellets of the same alloys (table 2) indicated that good dispersion was obtained.

TABLE 2. *Chromium content of mixed metal powders*

Alloy	Intended	Analyzed	
		Pellet 1	Pellet 2
	%	%	%
A	22.0	22.0	
B	18.0	18.0	18.1
C	14.0	13.9	13.9
D	22.0	21.7	21.7
E	14.0	13.9	14.0

The pellets were compacted and then sintered in dry hydrogen according to the following treatments:

240 hr at 2,500° F, then cooled in furnace; 1 hr elapsed between 2,500° and 1,500° F.

240 hr at 2,500° F, then cooled in furnace to room temperature at uniform rate in 30 hr; 12 hr elapsed between 2,500° and 1,500° F.

240 hr at 2,500° F, then cooled in furnace to 1,600° F; 1 hr elapsed between 2,500° and 1,600° F. The pellets were removed and allowed to cool to room temperature.

The condition of the alloys after sintering is referred to as "slow-cooled sintered." The variations in sintering treatments resulted from attempts to keep the furnace tube from cracking during the cooling operation. The long soaking period in dry hydrogen was a purification as well as a sintering treatment. The large initial oxygen content of the metal powders was beneficial because it made possible the oxidation and subsequent removal of the carbon contents of the powders.

Chemical analyses of randomly selected pellets were made to determine changes in composition of the alloys brought about by the sintering operation. These analyses showed that the average loss in chromium because of volatilization was 3.8 percent of the initial content. The chemical analysis for nickel and molybdenum was in good agreement with the charge analysis. Carbon contents were less than 0.01 percent. No carbides were observed in the microstructures or detected in residues, as shown by diffractometer charts. The oxygen contents of five samples were from 0.001 percent of oxygen for low chromium contents to 0.007 percent for high chromium contents. The nitrogen contents varied from 0.0023 to 0.0030 percent.

The losses indicated by these results were not considered sufficient to warrant correction of the charge analysis.

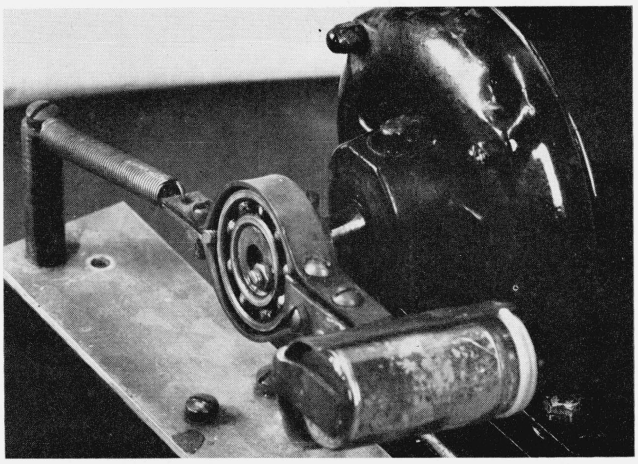

FIGURE 2. *Mixer and mixing jar for 30-gram charges.*

2.3. Approach to Thermal Equilibrium

Seven phases were encountered in studying the iron-chromium-molybdenum-nickel alloys and their derivative alloys. They were α Fe, γ Fe, σ, χ, epsilon (ϵ), eta (η), and rho (ρ) phases. The α Fe and γ Fe are terminal solution phases, and are referred to as soft phases to distinguish them from the intermediate σ, ϵ, χ, η, and ρ phases, which are hard and brittle. The ϵ phase has the composition Fe_3Mo_2 in the iron-molybdenum system. The compositions of the η and ρ phases were determined in this investigation, and their structures are discussed in section 3. The terminal molybdenum solid-solution phase was redesignated alpha-molybdenum (α Mo) in the contemporary diagram for the iron-molybdenum system [3] in order to indicate its structural relationship to α Fe, with which it forms a continuous solid-solution field in the iron-chromium-molybdenum-nickel system. Equilibrium could be approached either by precipitation of the hard phases or by re-solution.

Initially it was planned to approach equilibrium only by re-solution of the hard phases; that is, by reheating the slow-cooled sintered alloys in dry hydrogen to 2,200°, 2,000°, 1,800°, 1,650°, and 1,500°

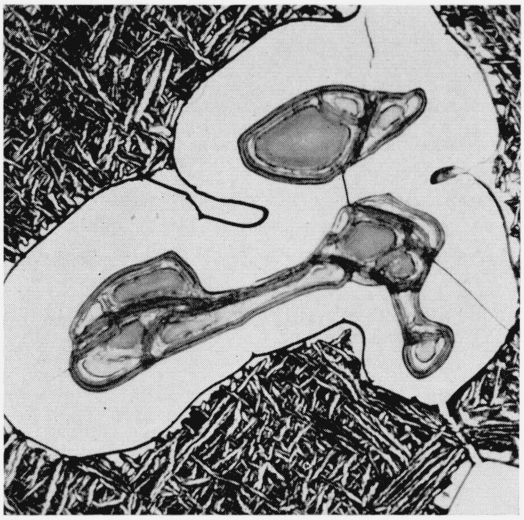

FIGURE 3. *Microstructure of alloy* 70 Fe-2 Cr-28 Mo *after reheating to 2,500° F for 2 hours and quenching in water.*

Concentrated hydrochloric acid containing few drops of nitric acid followed by 15 seconds in cold alkaline ferricyanide reagent. Phases identified were ϵ (dark) surrounded by ρ (white) in matrix (Widmanstätten structure) consisting of alternate bands of α and ρ. ×1000.

F for 25, 75, 250, 500, and 1,000 hr, respectively, and then quenching in water. Before reheating the alloys, those that were not brittle were compressed under 150,000- to 200,000-lb/in.^{2} pressure. This operation, by causing plastic deformation, reduced porosity and accelerated the reactions during the reheating periods. In the course of examining the reheated alloys, particularly those reheated at the lower temperatures, it was found that the microstructure of the hard phases had changed very little; and that, in a few alloys, the number of phases distinguished was more than could coexist if equilibrium had been established. Normally, according to Gibbs phase rule, the maximum number of phases in equilibrium at a temperature and pressure is 4 in a quaternary system, except when a phase transformation occurs; then there may be 5 or in the unique case 6. The foregoing observations indicated that, at the reheating temperatures, diffusion within the hard phases or from the hard phases to the matrix was slow; consequently, the approach to equilibrium was slow if several hard phases were involved. The shaded areas in figure 1 show the compositions in which the hard phases were found in the slow-cooled sintered alloys. The establishment of equilibrium in the alloys having compositions near the chromium-iron-molybdenum ternary system, particularly at high molybdenum contents, was doubtful, and the possibility of attaining equilibrium was even less at the lower temperature.

It was found that equilibrium could be approached more readily if the questionable slow-cooled sintered alloys were given a solution treatment prior to reheating to temperatures at which equilibrium was to be attained. The solution treatment consisted in reheating to 2,500° F, holding for 2 hr, and then quenching in water. In the solution-treated condition the alloys consisted of either or both the α Fe and γ Fe phases, except those alloys whose compositions were near the 30-percent-molybdenum corner of the diagram (fig. 1). These alloys contained traces of primary ϵ, ρ, or a fine acicular structure (fig. 3), which later was found to be ρ precipitated in a matrix of α Fe. The results as a whole indicated that the proximity of equilibrium was greater in a shorter period by precipitation from the soft phases than by reactions involving the hard phases. For the heating periods used in this work, it was only at 2,200° F that both the slow-cooled sintered and the solution-treated specimens gave consistent results.

In general, the boundaries between the areas containing the α and γ phases were considered to be accurate to $\pm$½-percent-alloy composition; the boundaries between the hard phases were considered to be less accurate.

2.4. Procedures for the Identification of Phases

The polishing procedure used in preparing the specimens for etching, preliminary to microscopic examination, was conventional except for the last stage, which consisted of either an electropolishing treatment or a combination of electrolytic and mechanical methods. The electrolyte consisted of 70 percent of glacial acetic acid, 20 percent of acetic anhydride, and 10 percent of perchloric acid (75% strength) by volume and was used at a potential between 40 and 50 v, dc. The most successful etching reagent was alkaline ferricyanide, made to the following strength: 20 g of $K_3Fe(CN)_6$ plus 20 g of KOH per 100 ml of water. This solution precipitated $K_3Fe(CN)_6$ at room temperature because of the common ion effect; but, inasmuch as satisfactory results were being obtained, no attempt was made to adjust its concentration.

The alkaline ferricyanide reagent was both staining and etching in its attack and was used either cold (room temperature) or hot (200° F). The sequence in which the interference colors appeared was approximately the same; however, the development periods of the colors differed considerably as a function of the temperature of the reagent. The final color of the film appeared to be copper brown, with variations of hue for different constituents. The σ phase required 2 or more min in the hot solution to acquire the brown film (figs. 4 and 5), whereas in a like period, η was deeply etched (fig. 5). Although not shown in this figure, ϵ also was deeply etched by the hot solution. In the cold solution, η and ϵ, when present, acquired a deep copper-brown film within 10 sec (figs. 6, 7, 8, and 9). The χ phase reacted slightly faster than σ but was sufficiently different to permit easy identification (figs. 4 and 5). The rate of staining of ρ was between that of η and χ (figs. 9, 10, and 11).

Primary α acquired a light-tan stain on prolonged etching in the hot alkaline-ferricyanide reagent, whereas γ or transformed γ was not affected (fig. 4). In specimens containing hard phases that were very sensitive to the hot reagent, primary α could be distinguished from primary γ or transformed γ either by previously etching with aqua regia (fig. 6) or by

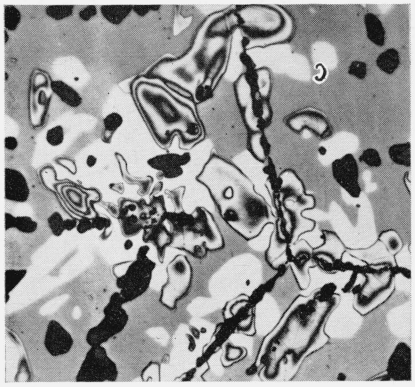

FIGURE 4. *Microstructure of alloy* 70 Fe-21 Cr-6 Mo-3 Ni *after reheating to 1,500° F for 500 hours.*

Two minutes in hot (200° F) alkaline ferricyanide reagent. Phases identified were α (light gray), γ (white), σ (nonuniformly stained), and χ (black). ×250.

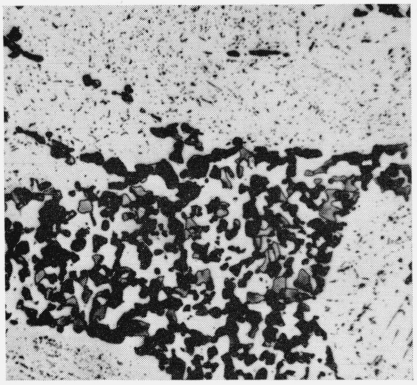

FIGURE 5. *Microstructure of alloy* 16.5 Cr-70 Fe-6.5 Ni-4 Mo *after reheating to 1,500° F for 500 hours.*

Stained 30 seconds in hot alkaline ferricyanide reagent. Phases identified were γ matrix, σ (gray), χ (black), and η (very small pitted constituent). Areas showing concentration of σ and χ were primary α at sintering temperature, those showing concentration of η and a trace of χ were primary γ. ×500.

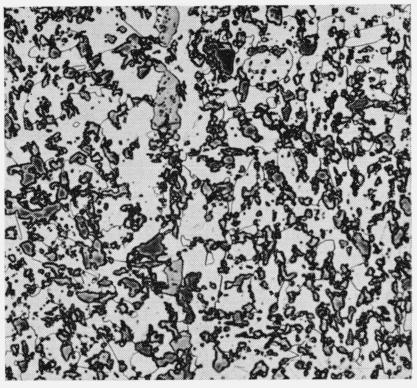

FIGURE 6. *Microstructure of alloy* 70 Fe-9 Cr-18 Mo-3 Ni *after reheating to 1,800° F for 250 hours.*

Aqua regia followed by 20 seconds in the cold alkaline ferricyanide reagent. Phases identified were α outlined in γ matrix, χ (light gray), and η (dark). ×250.

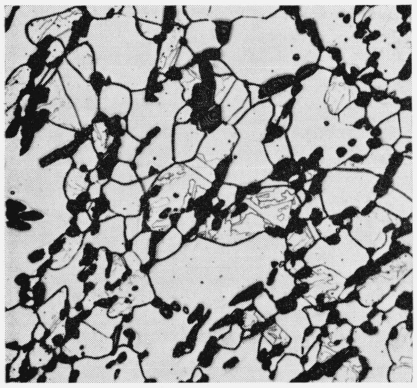

FIGURE 7. *Substructure in the* γ *phase. Alloy* 70 Fe-22.5 Mo-7.5 Ni *after reheating to 2,200° F for 25 hours.*

10-percent chromic acid electrolytically, followed by 10 seconds in cold alkaline ferricyanide. Phases identified were α (white), γ (white and substructure), and ϵ (dark). ×100.

FIGURE 8. *Substructure in the* γ *phase. Alloy* 70 Fe-26 Mo-4 Ni *after reheating to 2,000° F for 75 hours.*

10-percent chromic acid electrolytically, followed by 10 seconds in cold alkaline ferricyanide. Phases identified were α (white), γ (white with substructure), and ϵ (dark). ×500.

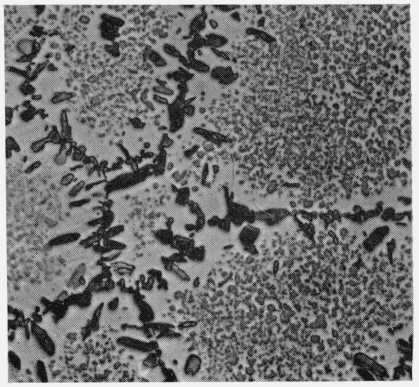

FIGURE 9. *Microstructure of alloy* 70 Fe-2 Cr-28 Mo *after reheating to 2,200° F for 25 hours.*

10 seconds in alkaline ferricyanide reagent. Phases identified were α matrix with ρ (speckled) within the network formed by ϵ (black). ×100.

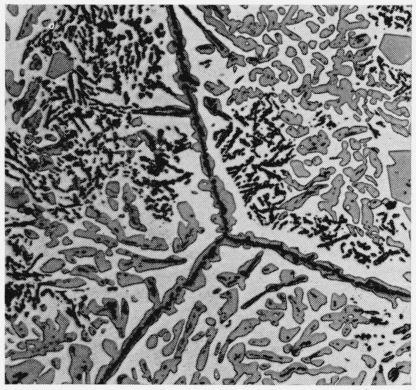

FIGURE 10. *Microstructure of alloy* 70 Fe-9 Cr-21 Mo *after reheating to 2,000° F for 75 hours.*

Aqua regia followed by 20 seconds in cold alkaline ferricyanide reagent. Phases identified were α matrix containing χ (light gray) and ρ (black). ×100.

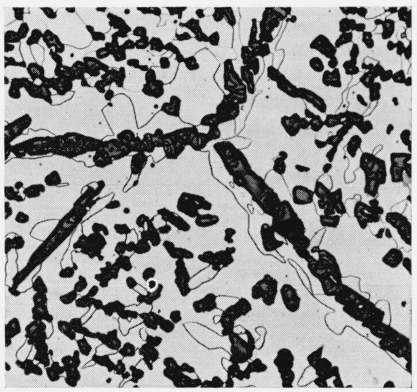

FIGURE 11. *Microstructure of alloy* 70 Fe-4 Cr-22 Mo-4 Ni *after reheating to 2,000° F for 75 hours.*

10-percent chromic acid electrolytically followed by 30 seconds in hot alkaline ferricyanide reagent. Phases identified were α matrix containing γ (outlined and unstained), and ρ (dark). ×250.

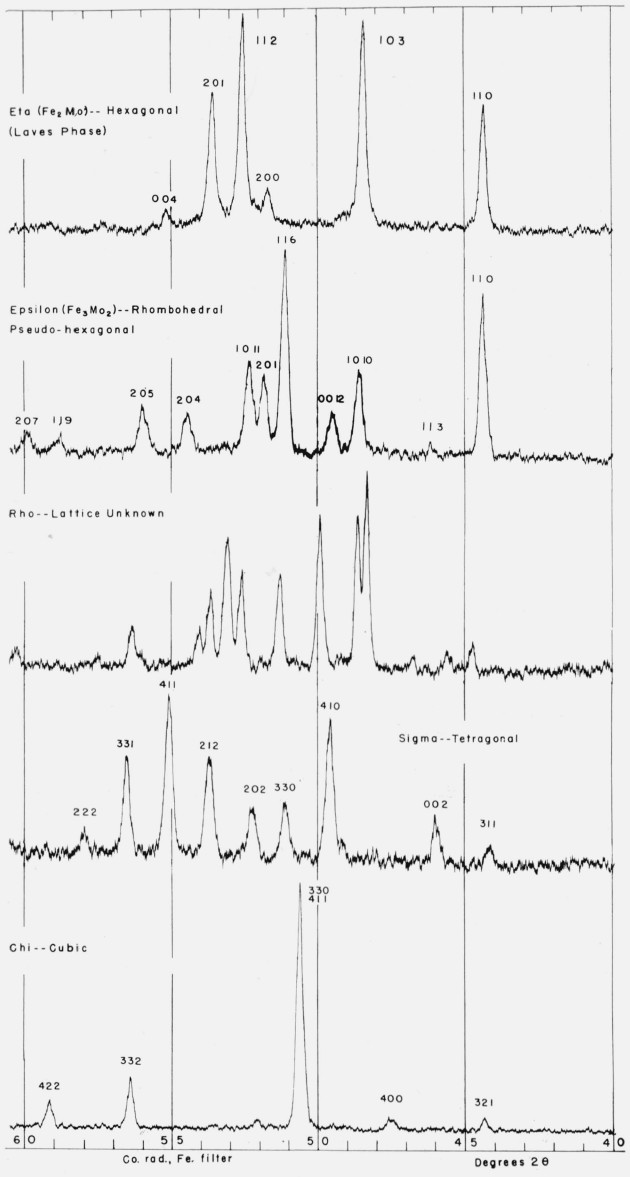

FIGURE 12. *Diffractometer charts of the hard phases* χ, η, ϵ, ρ, *and* θ.

electrolytically etching in 10-percent chromic acid (figs. 7, 8, and 11). The η and ϵ phases could not be readily distinguished from each other. The rates of attack or staining of the hard constituents varied somewhat with alloy composition and reheating temperature; but this change was gradual and did not affect the ease of identification.

The most rapid change in the effects of the alkaline-ferricyanide reagent on σ occurs in alloys whose molybdenum contents varied from 0 to 3 percent, which include the commercial alloys. This rapid change, however, did not affect the certainty with which σ could be distinguished. The rapid change in the action of the alkaline-ferricyanide reagent on σ probably is explained by the rapid change in the molybdenum content of σ in alloys varying from 0 to 3 percent, for it has been found [2] that σ in a 3.2-percent-molybdenum commercial alloy contains approximately 12 percent of molybdenum.

The phases distinguished in the microstructure were carefully correlated with their respective X-ray diffraction patterns. This was possible to a large extent because, with respect to the soft phases (α Fe and γ Fe), the hard phases (σ, χ, ϵ, ρ, η) were relatively insoluble in the following solutions:

Dissolution procedure:

45 g of $FeCl_3 \cdot 6H_2O$ in 100 ml of water. Used largely for specimens low in chromium that had been reheated to 1,800° F or lower.

100 ml of HCl concentrated, plus 1 or 2 drops of nitric acid. Used to separate η.

10 g of $CuCl_2$ in 100 ml of HCl, concentrated. Used largely for specimens reheated to 1,800° F or lower temperatures.

Aqua regia. Used to separate σ and χ.

Electrolytic dissolution procedure:

45 g of $FeCl_3 \cdot 6H_2O$ in 100 ml of water. Used to separate σ and χ.

10 percent HCl. Used to separate χ, ϵ, η, and ρ.

The correlations were made by selecting alloys that contained a single hard phase, making a thorough study of their microstructures, and then obtaining a diffractometer chart from each of the separated hard phases. Analyses of these charts showed that each phase had a characteristic pattern that could be easily identified in the 2θ range of 40° to 60° (Co–Kα radiation) of the diffractometer, as shown in figure 12.

Diffraction charts obtained from residues containing several phases were sometimes troublesome to analyze because of superposition of lines, particularly when residues contained only traces of phases; for example, when η was present as a trace in a mixture of ρ and ϵ. Recourse to angles beyond the 40° to 60° diffractometer range did not help, because too many lines overlapped or were too weak to be resolved. In these cases identification usually could be made by the judicious use of solutions listed above. The solubility of the hard phases differed slightly in the different solutions, thereby affecting the relative amounts of the phases in the residue. This affected the relative intensities of lines belonging to certain patterns, thus aiding in their separation and the subsequent identification of the patterns registered on the diffractometer chart.

There were a few cases in which it was difficult to distinguish microscopically between certain hard and soft phases. In those cases corroborating evidence was obtained from the diamond pyramid hardness (DPH) values on the phases in question. For this purpose a Bergsman hardness tester was employed, using a 15-g load for 10 sec. The DPH values for the soft phases varied from 200 to 400, and the hard phases, from 1,000 to 2,000, no attempt was made to distinguish between certain hard and soft phases.

3. Structure of Phases

Because all of the five hard phases encountered in the 70-percent-iron quaternary alloys can be represented in a chromium-iron-molybdenum ternary diagram, this type of diagram, without regard for temperature, has been used to represent their approximate composition (fig. 13).

The well-known σ phase has a tetragonal structure [4], and in the chromium-iron system σ has the composition of FeCr, and is stable below 1,508° F [5]. If considered on a temperature gradient, σ has a solid-solution field [6,7] through the chromium-iron-molybdenum ternary to the chemical composition FeMo [8,9] in the iron-molybdenum system, where it is stable only above 2,160° F [10].

The χ phase [11] has a low-symmetry cubic structure of the alpha-manganese type and a chemical formula, $Fe_{36}Cr_{12}Mo_{10}$ [12,13]. Results of this investigation, discussed later, indicate that χ has an upper limit of stability at approximately 2,150° F.

The ϵ phase has a rhombohedral structure [14,15], and the chemical composition Fe_3Mo_2 [7,8,16]. The ϵ phase can dissolve considerable nickel [17] but very little chromium.

The η phase was found, early in the work in residues separated from the quaternary alloys, to have a hexagonal structure. This suggested that the structure of η was the Laves type and isomorphic with that of Fe_2W [15]. Kuo [18], in discussing VerSnyder's and Beattie's paper [19], in which they report a phase of the Laves type in a modified 12-percent-chromium stainless alloy, pointed out that Zaletaeva, et al. [20] had reported recently the existence of Fe_2Mo. Zaletaeva found a hard phase in a 0.1-percent-carbon, 16-percent-chromium, 25-percent-nickel, 6-percent-molybdenum alloy that was considered to be Fe_2Mo, but this was not confirmed by chemical analysis. Kuo also gave additional indirect evidence of the existence of Fe_2Mo. These reports are in line with the early work of Vigoroux [21], who had reported Fe_2Mo on the basis of chemical analysis of residues obtained from alloys made by reducing mixtures of iron and molybdenum oxides.

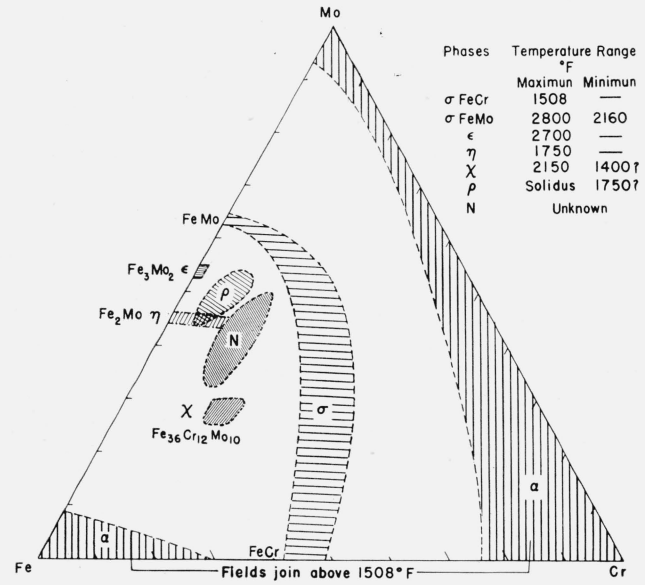

FIGURE 13. *Schematic representation of the compositions of the hard phases in the chromium-iron-molybdenum system.*

The foregoing review definitely indicated the existence of a Fe_2Mo phase, notwithstanding the fact that it is not included in the contemporary diagram [3]. In order to determine whether or not FeMo, Fe_3Mo_2, and Fe_2Mo could be made by powder technique and to provide standard diffraction patterns of the ϵ and η phases, several iron-molybdenum alloys were investigated.

Iron-molybdenum alloys having compositions of FeMo, Fe_3Mo_2, and Fe_2Mo were prepared and sintered. Alloys FeMo and Fe_3Mo_2 were reheated to 2,690° F for 2 hr and quenched in water. Alloy Fe_2Mo was heated to 2,500° F for 2 hr and quenched in water. Specimens then were reheated to 2,200°, 2,000°, 1,800°, 1,650°, and 1,500° F, as previously described. The phases indicated by diffraction patterns obtained from the reheated specimens are listed in table 3. The FeMo alloy quenched from 2,690° F was σ, but was ϵ and α Mo when quenched from 2,200° F. This indicates that FeMo decomposes at a higher temperature than indicated by the iron-molybdenum diagram, providing the alloy did not transform in quenching. The Fe_3Mo_2 alloy quenched from 2,690° F was σ with a trace of ϵ, but was ϵ when quenched from 2,200° and 2,000° F. The Fe_2Mo alloy quenched from 2,500° and 2,200° F was α and ϵ, but was α, ϵ, and η when quenched from 1,500° F. Obviously equilibrium was not established, but the results did indicate that at 1,500° F, α, and ϵ were reacting to form η and that η was not stable at 2,000° F. In order to establish better the existence of Fe_2Mo and to provide an alloy from which it could be separated with minimum contamination, an alloy having the composition 80-percent-iron and 20-percent-molybdenum was prepared, sintered, and soltion-treated at 2,500° F. Quenched from 2,500° F, this alloy was α; from 2,200° and 2,000° F, α and ϵ; from 1,800° F, α, ϵ, and η; and from 1,650° and 1,500° F, α and η. Equilibrium was not established at 1,800° F, probably because the upper temperature of stability of η is near 1,800° F.

TABLE 3. *Phases identified in iron-molybdenum alloys*

Atom ratio	Mo content	Reaction temperature, °F					
		2,500	2,200	2,000	1,800	1,650	1,500
	Weight %						
FeMo	63	[a]	ϵ, α Mo				
Fe_3Mo_2	55	[b]	ϵ	ϵ	----	----	----
Fe_2Mo	46.2	α, ϵ	α, ϵ	α, ϵ	----	----	α, ϵ, η
	20	α, ϵ	α, ϵ	α, ϵ	α, ϵ, η	α, η	α, η

[a] Reheated to 2,690° F for 2 hr, and quenched in water. Examination showed σ.

[b] Reheated to 2,690° F for 2 hr, and quenched in water. Examination showed σ and trace of ϵ.

TABLE 4. *Data obtained from standard X-ray diffraction pattern for the ϵ phase,*[a] Fe_3Mo_2

hkl	*d*	*I* [b]	2θ (Co-Kα radiation)	*hkl*	*d*	*I* [b]	2θ (Co-Kα radiation)
	A		*deg*		*A*		*deg*
104	3.46	6	30.00	1·0·20	1.2258	6	93.72
110	2.373	90	44.33	1·1·18	1.2231	25	93.99
113	2.289	4	46.05	0·0·21			
1·0·10	2.179	67	48.51	2·0·17	1.2176	15	94.55
0·0·12	2.141	20	49.43	220	1.1870	25	97.79
116	2.077	100	51.08	2·0·20	1.0894	10	110.39
201	2.050	42	51.79	1·1·21	1.0874	18	110.69
202	2.031	52	52.30	2·1·17	1.0834	4	111.29
1·0·11				0·0·24	1.0704	5	113.36
204	1.958	20	54.40	3·0·15			
205	1.910	32	55.90	3·1·10	1.0424	23	118.20
119	1.825	9	[c] 58.74	2·2·12	1.0384	12	118.99
207	1.794	9	59.82	401	1.0274	4	121.05
1·0·13	1.781	4	60.36	3·1·11	1.0249	18	121.56
208	1.732	3	62.20	402			
2·0·10	1.605	4	67.73	2·0·22	1.0154	8	123.50
1·0·16	1.495	2	73.50	404			
1·0·17	1.4182	2	78.20	405	1.0082	6	125.05
1·1·15	1.3889	4	80.18	407	0.9902	6	129.19
300	1.3706	17	81.47	3·0·18	.9885	11	129.62
2·1·10	1.3296	25	84.55	4·0·10	.9546	3	139.10
306	1.3052	23	86.52	2·2·18	.9128	19	157.00
2·1·11	1.2939	22	87.46	3·0·21			
2·0·16	1.2652	13	89.98	2·1·23	.9071	5	160.86

Lattice parameters

Hexagonal system: $a=4.748_6$ A, $c=25.68_6$ A, and $c/a=5.409$.
Rhombohedral system: $a=8.99_{02}$ A, $\alpha=30°37.6'$.

[a] Separated from 80 Fe–20 Mo alloy after reheating to 2,000° F for 75 hr. The α Fe matrix was dissolved electrolytically in a 10-percent HCl solution.
[b] The relative height of peak in the diffractometer chart obtained with Co-Kα radiation with respect to strongest line.
[c] All angles greater than 58.74 deg are to the peak of the Co-Kα$_1$ wavelength.

The lattice parameters calculated from the data obtained from diffraction charts for the ϵ that had been separated from the 80-percent-iron, 20-percent-molybdenum alloy after reheating to 2,000° F (table 4) compare very well with the values, $a=4.741$ A and $c=25.63$ A, reported by Arnfelt and Westgren [15]. The excellent agreement of the observed intensities, obtained for η from the residue after reheating to 1,650° F, with the calculated intensities obtained by VerSnyder and Beattie (table 5), is considered to confirm that Fe_2Mo does exist and that it has the Laves $MgZn_2$ type of structure. Chemical analysis of the separated η (table 6) indicates that Fe_2Mo can dissolve up to 4 percent of iron at 1,650° F. Similar analyses of η separated from the quaternary alloys indicate that nickel and chromium also are soluble in the structure.

The ρ phase, obtained from a quaternary alloy containing 1 percent of nickel, was identified as having a composition of approximately 4 percent of chromium, 53 percent of iron, and 43 percent of molybdenum (table 6); but as yet the structure is unknown. This composition has been confirmed by specially prepared alloys (table 7), which also indicate that ρ has an increased solubility field near the solidus. The *d*-spacing of ρ showed a pronounced shift to larger values with the addition of molybdenum. The iron-rich composition approximates the type formula AB_2 of the Laves structure, considering molybdenum as the A unit and iron and chromium as the B unit. This inference proved to be improbable, however, because the *d*-spacings (table 7) did not correspond to a hexagonal structure of the Laves type.

Goldschmidt [22] has reported an "N" phase in the chromium-iron-molybdenum system with a solubility field at approximately 1,100° F, as shown in figure 12. The diffraction data for N [12] did

TABLE 5. *Data obtained from standard X-ray diffraction pattern for the η phase,*[a] Fe_2Mo

hkl	*d*	*I*		2θ (Co-Kα$_1$ radiation)
		Observed [c]	Calculated [d]	
	A			*deg*
100	4.100	2	0.6	25.20
101	3.624	3	3.6	28.58
102	2.812	6	7.0	37.09
110	2.369	56	56.7	44.37
103	2.180	100	101.0	48.44
200	2.053	16	14.6	51.67
112	2.020	93	100.0	52.57
201	1.984	68	73.2	53.60
004	1.931	7	9.6	55.19
202	1.813	3	5.9	59.14
104	1.7478	6	8.4	61.56
203	1.6047	1	0.3	67.75
211	1.5217	0.5	.5	72.00
105	1.4464	8	4.1	76.40
300	1.3689	9	6.4	81.60
213	1.3294	50	24.5	84.57
302	1.2906	20	17.8	87.57
006	1.2876	10		88.00
205	1.2349	20	18.3	92.82
106	1.2286	4	2.4	93.44
214	1.2103	1	3.4	95.30
220	1.1859	16	14.9	97.92
215	1.0954	7	2.4	109.49
312	1.0930	5	0.4	109.84
206	1.0911	5	5.8	110.13
313	1.0421	15	9.1	118.26
401	1.0182	3	------	122.93
224	1.0107	3	------	124.51
402	0.9198	2	------	128.64
216	.9912	2	------	128.98
108	.9402	14	------	144.12
315	.9171	4	------	154.48
410 [b]	.8966	------	------	172.090

Lattice parameters

Hexagonal system: $a=4.744_2$A, $c=7.725_7$A, $c/a=1.628$.

[a] Separated from 80 Fe-20 Mo alloy, after reheating to 1,650° F for 500 hr. The α Fe matrix was dissolved electrolytically in a 10-percent HCl solution.
[b] Data obtained from pattern of back-reflection focusing camera.
[c] The relative height of peak in the diffractometer chart obtained with Co-Kα radiation with respect to strongest line.
[d] Data taken from VerSynder and Beattie, Trans. Am. Soc. Metals **47**, p. 219 (1955).

TABLE 6. *Chemical analysis of single-phase residues*

Temperature	Parent alloy (%)				Residue (%)				Phase
	Cr	Fe	Mo	Ni	Cr	Fe [a]	Mo	Ni	
° *F*									
1,650	0	80	20	0	0	55.8	44.2	0	η
1,650	4	70	8	18	2.8	47.2	46.0	4.0	η
1,650	9	70	12	9	6.0	45.5	44.4	4.1	η
1,800	4	70	25	1	3.8	52.7	43.5	0	ρ

[a] By difference.

TABLE 7. *Phases identified in* Cr-Fe-Mo *alloys containing less than 70 percent of iron*

Cr	Fe	Mo	Reaction temperature (° F)					
			2,500	2,200	2,000	1,800	1,650	1,500
%	%	%						
16.5	53.1	30.4	α, σ	α, σ	χ,[b] t A	χ,tA	χ,tA	χ,tA
5	48.5	[a] 46.5	ρ	ρ	ρ, ϵ	ρ, ϵ	----	ρ
10	43	[a] 47	ρ	ρ, ϵ	ρ, ϵ	ρ	----	ρ
5	55	40	α, ρ	α, ρ	α, ρ	α, ρ	----	----
10	58	32	α, ρ	α, ρ	α, ρ, χ	α, ρ, χ	----	χ, A
5	42	[a] 53	ρ	ϵ	ϵ	ϵ	η	----
10	40	[a] 50	ρ	ρ	ρ, tϵ	ϵ	ρ	----
5	51	[a] 44	ρ	ρ	ρ	ρ	ρ, A	----
			2,600	2,200	2,150	2,125	2,100	1,500
18	56	26	α	α, σ	α, σ, tχ	χ, tσ	χ	χ

[a] X-ray diffraction data only.
[b] t, traces; A, other unidentified phase or phases present.

not agree with that for ρ (table 8). Goldschmidt [23], in referring to unpublished work, stated that N was isomorphic with a phase in the chromium-cobalt-molybdenum system that has the approximate formula $Co_5Cr_3Mo_2$. Rideout and Beck [24,25] reported an "R" phase at the approximate composition of $Co_{10}Cr_4Mo_7$. If cobalt and chromium are considered the B unit, R also approximates the AB_2 type formula. The diffraction pattern of R differs from that of the N phase. Except for a few weak lines, there is excellent agreement of the R lines with those of the ρ phase (table 8). The presence of ρ in the chromium-iron-molybdenum system is not incompatible with that of N, but the results for the former do indicate that N is not stable at temperatures above 1,500° F. Alloys at lower temperatures were not investigated.

The ρ phase has been found to precipitate in 70-percent-iron ternary and quaternary alloys having

TABLE 8. *Data obtained from standard X-ray diffraction pattern for* ρ[a] *and similar data for the R phase [23,24] in the* Co-Cr-Mo *system*

ρ phase			R phase		ρ phase			R phase	
d	I/I_0[b]	2θ (Co-Kα radiation)	d	I[d]	d	I/I_0[b]	2θ (Co-Kα radiation)	d	I[d]
A		*deg*			*A*		*deg*		
3.36	10	30.92			1.2451	13	91.84		
2.83	9	36.92			1.2403	29	92.29	1.231	w
2.78	6	37.58			1.2331	7	93.00		
			2.659	w	1.2289	28	93.41	1.219	w
2.63	7	39.80	2.612	vw	1.2244	7	93.86		
			2.592	vw	1.2163	10	94.68		
			2.529	vvw	1.2138	11	94.94	1.207	w
			2.473	w	1.2117	7	95.15		
2.351	15	44.74	2.337	w	1.2088	8	95.45		
2.310	10	45.60	2.291	w	1.1952	6	96.90		
2.258	8	46.72	2.238	vw	1.1776	5	98.85		
			2.186	w	1.1747	6	99.18		
2.189	100	48.27	2.171	s	1.1585	9	101.08		
2.176	80	48.59	2.159	s	1.1559	11	[e] 101.40		
2.151	6	49.18			1.1432	5	102.96		
2.122	80	49.90	2.106	ms	1.0980	16	109.01		
2.069	59	51.27	2.052	ms	1.0911	11	110.12		
2.020	48	52.59	2.005	s	1.0822	15	111.58		
2.003	76	53.08	1.987	ms	1.0736	16	112.84		
1.984	41	53.64	1.966	ms	1.0687	11	113.63		
1.971	22	54.05	1.954	m	1.0616	14	114.82		
			1.890	vw	1.0450	6	117.73		
1.896	30	56.33	1.881	w	1.0091	11	124.84		
1.860	9	57.52	1.849	vw	0.9959	8	127.83		
1.784	15	60.22	1.770	mw	.9942	13	128.24		
1.742	8	61.82			.9910	7	129.00		
1.505	5	73.05			.9890	6	[e] 129.48		
1.479	6	74.52			.9835	6	130.86		
1.430	7	77.52			.9757	7	132.80		
1.420	4	78.14			.9739	11	133.40		
1.414	5	78.60			.9722	8	133.90		
1.392	5	[c] 79.98			.9678	5	135.10		
1.383	3	80.60			.9631	12	136.48		
1.373	15	81.27			.9606	8	137.24		
1.368	11	81.68			.9582	7	137.96		
1.351	9	82.89			.9539	4	139.34		
1.304	14	86.60	1.291	vw	.9447	8	144.64		
1.2903	31	87.77	1.280	w	.9256	7	150.20		
1.2896	25	87.83			.9175	7	154.25		
1.2827	6	88.42			.9127	6	157.06		
1.2785	29	88.79	1.268	mw	.9093	6	159.28		
1.2728	28	89.29	1.263	w	.9062	4	161.50		
1.2555	30	90.86	1.246	vw	.9027	22	164.50		

[a] Separated from 4 Cr-70 Fe-26 Mo alloy after reheating to 2,500° F for 2 hr, quenching in water, and reheating to 2,200° F for 25 hr. The αFe matrix was dissolved electrolytically in a 10-percent HCl solution.
[b] The relative height of peak in the diffractometer chart obtained with Co-Kα radiation with respect to strongest line.
[c] All angles greater than 78.60° are to the peak of the Co-$K\alpha_1$ wavelength.
[d] s, Strong; ms, medium strong; m, medium; mw, medium weak; w, weak; vw, very weak; vvw, very very weak.
[e] Probably high because of superposition of the Co-$K\alpha_2$ wavelength.

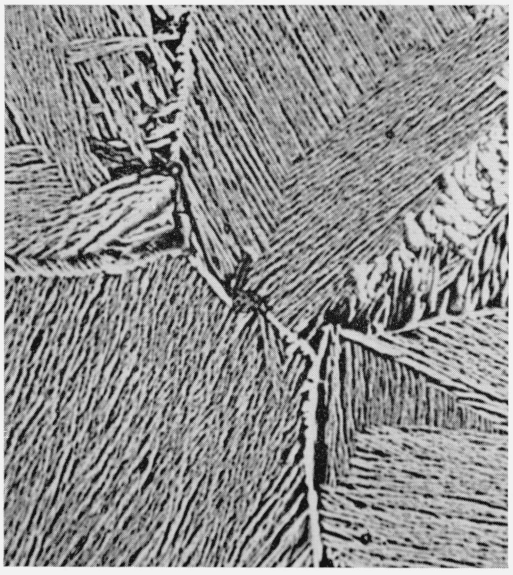

FIGURE 14. *Microstructure of* 65 Fe-35 Mo *alloy after reheating within liquidus, 2,675°F, and quenching in water.*

Concentrated (hydrochloric acid) containing few drops of nitric acid. Shows characteristic Widmanstätten structure. X-ray diffractometer chart obtained from polished surface indicated that α and ρ were present. ×1500.

approximately 30 percent of molybdenum on quenching from the sintering temperature. This suggests that the precipitation observed by earlier workers [8,10,16] in the iron-molybdenum binary alloys might be ρ. An alloy containing 65 percent of iron and 35 percent of molybdenum when quenched from the melt, was found to contain α and ρ by X-ray diffraction methods. The microstructure (fig. 14) indicates that upon solidification, α formed first and then ρ precipitated forming the Widmanstätten structure. The ρ phase appears to be transitory or metastable in iron-molybdenum binary and iron-molybdenum-nickel ternary alloys, somewhat analogous to γ' in the silver-aluminum system [26]; therefore, ρ should not be indicated in the phase diagrams of these systems.

4. Phase Diagrams

4.1. The Iron-Molybdenum System

The contemporary phase diagram for the iron-molybdenum system [3] was modified to include the

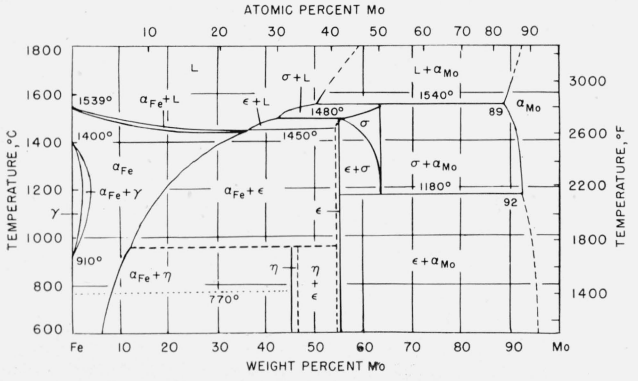

FIGURE 15. *Contemporary phase diagram of the iron-molybdenum system modified to show the* η *phase.*

Fe_2Mo phase that has been tentatively designated as η (fig. 15). The field for FeMo was redesignated as σ to conform with present knowledge.

4.2. The Iron-Chromium-Molybdenum Alloys Containing 70 and 80 Percent of Iron

The information obtained from a survey of the literature on the chromium-iron-molybdenum system was summarized in temperature-composition diagrams (figs. 16 and 17) for comparison with the results in this investigation (figs. 18 and 19). Putman, et al. [6] and Baen and Duwez [7] indicated extensive fields containing σ, whereas McMullin, et al. [12] indicated that this area contained χ and only small fields containing σ. Goldschmidt [22], in addition to fields containing ϵ and σ at 1,090° F, indicated other fields that included the N phase previously discussed.

From the results for the 70-percent-iron alloys (fig. 18), it was concluded that there were fields containing ρ at high temperatures. The upper limit of χ is indicated at approximately 2,150° F. This was justified by the absence of χ, in alloys containing 15.5, 18, 19.5, and 22.5 percent of molybdenum, after reheating to 2,200° F and on the basis of results obtained with an alloy that corresponded to the composition of χ [12]. These results (table 7) showed χ was present at 2,150° F but not at 2,200° F. The presence of α plus σ at 2,200° and 2,150° F, and χ plus σ at 2,125° F, indicates that the 18-percent-chromium, 56-percent-iron, and 26-percent-molybdenum alloy cuts across mono- and bi-phase fields in the range from 1,500° to 2,600° F.

A horizontal line was drawn slightly below 1,800° F to indicate the lower limit of ϵ; however, it is believed that the lower limit of ρ is better represented by the eutectoid type of decomposition (fig. 18). This section of the diagram is considered to be tentative because of the difficulty in approximating equilibrium in alloys containing 22.5 to 28 percent of molybdenum. The boundaries of fields containing χ were not extrapolated below 1,500° F because there is evidence that χ might have a lower limit of stability. The χ phase was not observed in the alloy having the χ composition when reheated for 16 hr at 1,400° F; furthermore, only traces of χ and large amounts of η were found in the 70-percent-iron alloys, having compositions in the χ area outlined in figure 1, that were examined after the sintering treatments. In the sintering treatments the cooling rate was rapid between 2,500° and 1,500° F. The boundary between the α and α-plus-σ fields was connected to the point in the chromium-iron system indicated in the diagram by Cook and Jones [5]. The connecting curve appears reasonable.

The results of examinations of the iron-chromium-molybdenum alloys containing 80 percent of iron are summarized in figure 19 and appear consistent with those obtained for the 70-percent-iron alloys. The iron-chromium-molybdenum alloys containing 80 percent of iron were prepared to help interpret and substantiate the results for the 70-percent-iron alloys, particularly those alloys whose composition

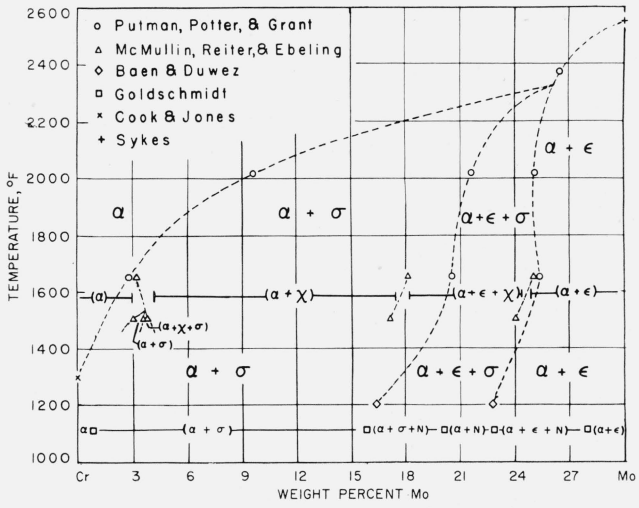

FIGURE 16. *Temperature-composition diagram for iron-chromium-molybdenum alloys containing 70 percent of iron.*
Constructed from data in published reports.

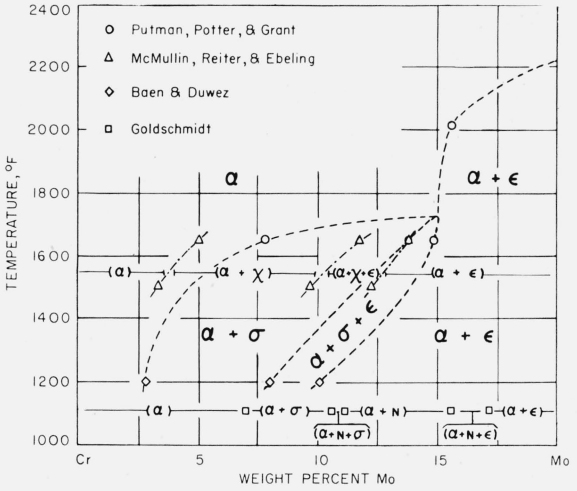

FIGURE 17. *Temperature-composition diagram for iron-chromium-molybdenum alloys containing 80 percent of iron.*
Constructed from data in published reports.

was near the 30-percent-molybdenum corner. They also helped in interpreting results obtained at the lower temperatures, 1,800°, 1,650°, and 1,500° F. The results obtained for the high-molybdenum–70-percent–iron alloys had shown that the hard phases precipitated during cooling from the sintering operation had not changed when reheated to 1,800° F or below. These alloys, when solution-treated for 2 hr at 2,500° F, precipitated finely divided ρ in quenching or in the initial stages of there heating periods. Furthermore, the end products involved in reactions between the finely divided precipitates and the matrix at the reheating temperatures were difficult to resolve and distinguish in the microstructure. In some specimens it appeared that the finely divided ρ had not decomposed, and moreover, the lines in the diffraction patterns were diffuse. These difficulties were not experienced in the high-molybdenum–80-percent–iron alloys. The microstructure could be interpreted and the diffraction patterns were better

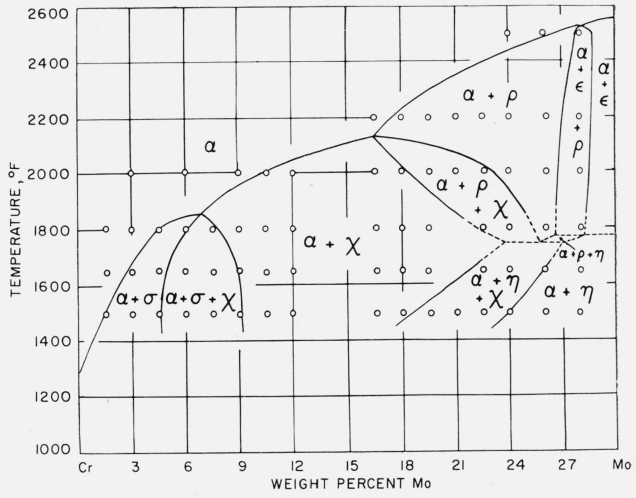

FIGURE 18. *Temperature-composition diagram for iron-chromium-molybdenum alloys containing 70 percent of iron.*
Open circles indicate alloys investigated.

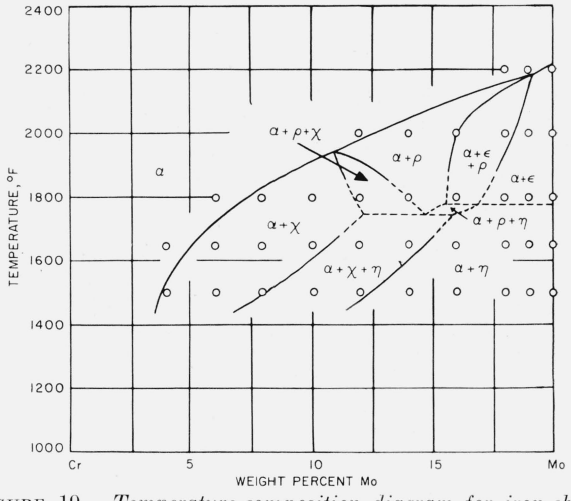

FIGURE 19. *Temperature-composition diagram for iron-chromium-molybdenum alloys containing 80 percent of iron.*
Open circles indicate alloys investigated.

defined. Equilibrium probably was closely approximated at all temperatures except possibly at 1,800° F.

4.3. The Iron-Molybdenum-Nickel Alloys Containing 70 Percent of Iron

The phases identified in the iron-molybdenum-nickel alloys are summarized graphically in a temperature-composition diagram, figure 20. The information in the literature is limited to an investigation by Das and Beck [17] at 2,200° F and the contemporary iron-molybdenum diagram by Sykes [3]. The present work indicates that the boundary between the γ-plus-ϵ and γ fields is at 18 percent of nickel rather than 15.5 percent of nickel, as indicated by Das and Beck. The boundaries encompassing the γ-plus-η-plus-ϵ field are less certain than the other boundaries and are dashed. Results obtained for iron-molybdenum-nickel alloys having iron contents other than 70 percent of iron (table 7) indicated

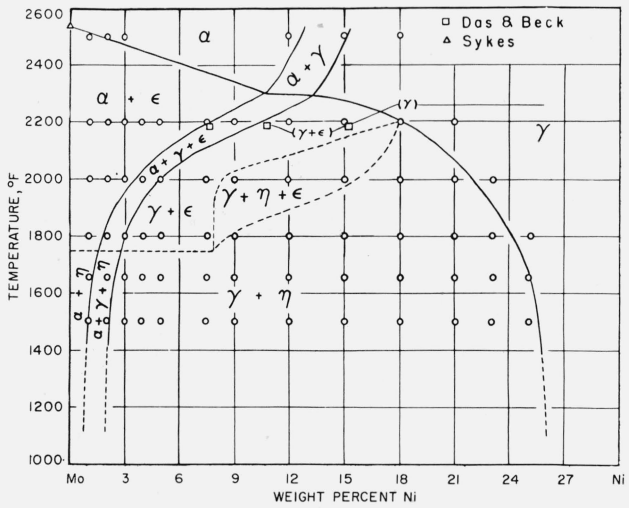

FIGURE 20. *Temperature-composition diagram for iron-molybdenum-nickel alloys containing 70 percent of iron.*

Open circles indicate alloys investigated. The open squares and triangles are points taken from published reports.

that the duration of the sintering treatment might influence the relative amounts of ϵ and η formed at the reheating temperature. The ϵ phase was found in instances when η was expected in a few alloys in which the sintering period had been 48 hr instead of the customary 240 hr. A probable explanation of these results is that oxygen was not so completely removed as in the 240-hr sintering treatment. The oxide particles probably retarded or prevented the reaction in which η is formed at the expense of ϵ.

4.4. The Iron-Chromium-Nickel Alloys Containing 70 Percent of Iron

The phases identified in the iron-chromium-nickel alloys and information derived from the literature are summarized in figure 21. The agreement between the results of the present study and those of Rees, et al. [27] are very good, but quite different from those of Schafmeister and Ergang [28]. The

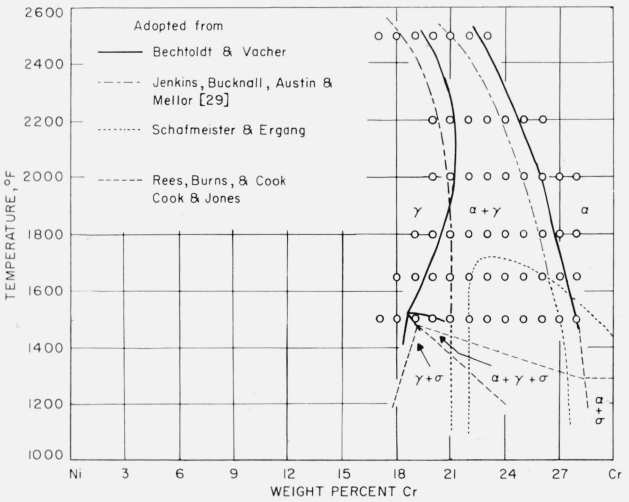

FIGURE 21. *Temperature-composition diagram for iron-chromium-nickel alloys containing 70 percent of iron.*

junction of the γ, γ-plus-σ, α-plus-γ, and α-plus-γ-plus-σ fields is shown to be 0.5 percent toward higher nickel contents, and 30° to 40° F higher in temperature than that indicated by data from Rees, et al.

4.5. The Iron-Chromium-Molybdenum-Nickel Alloys Containing 70 Percent of Iron

The alloy compositional limits of the seven phases, α, γ, σ, ϵ, χ, η, and ρ, in the 70-percent-iron alloys at the 5 temperatures of 2,200°, 2,000°, 1,800°, 1,650°, and 1,500° F are shown graphically in 5 ternary diagrams, figure 22. The apexes are points in the corresponding binary systems, and the sides are isothermal sections in figures 18, 20, and 21.

The hard phases occur only near the 30-percent-molybdenum corner at 2,200° F. It is probable that the hard phases would not be present in the 70-percent-iron alloys at approximately 2,530° F; therefore, a similar diagram would show only the compositional limits of α and γ. There are definite areas for ρ and ϵ at 2,200° F. The area in which η was found is less certain. It is probable that η is stable at a higher temperature in the quaternary alloys than in the ternary and binary alloys.

At 2,000° F, χ was found and the field in which η was found was expanded considerably. Fields for all seven phases were found at 1,800° F. The σ phase is represented in two separate areas. This was checked with alloys that had compositions lying between the stable areas. It is probable that in alloys of lower iron content, the σ areas would be connected.

The ϵ and ρ phases were not found in the 70-percent-iron quaternary alloys at 1,650° and 1,500° F. The area in which σ was found has continued to expand, and at 1,500° touches the 70-percent-iron–molybdenum-nickel ternary line. It is noteworthy that the minimum chromium content of the σ areas is about 16 percent for a range of 3 to 9 percent of molybdenum at 1,800°, 1,650°, and 1,500° F. Because some alloys within the σ areas are mixtures of α and γ in varying ratios at temperatures near 2,500° F; and because σ, and χ to a lesser extent, preferentially precipitates in primary α [2]; and because η apparently prefers primary γ (fig. 5), the boundaries of these areas in which σ, χ, and η are found might be influenced by the solution-treating temperature. The total shift in a boundary that could be brought about by changes in the relative amounts of primary α and γ is believed to be less than 2 percent in alloy composition.

The evidence that χ probably was not stable below 1,500° F was discussed in a previous section. A diagram at such a temperature would show only α, γ, σ, and η. The boundary of the area in which η would be found probably would start at 3 to 6 percent of molybdenum in the 70-percent-iron–chromium-molybdenum ternary line, connect with the η area as shown in the 1,500° F diagram at 20 percent of chromium and 3 percent of molybdenum, and continue as drawn to the 70-percent-iron–molybdenum-nickel ternary line.

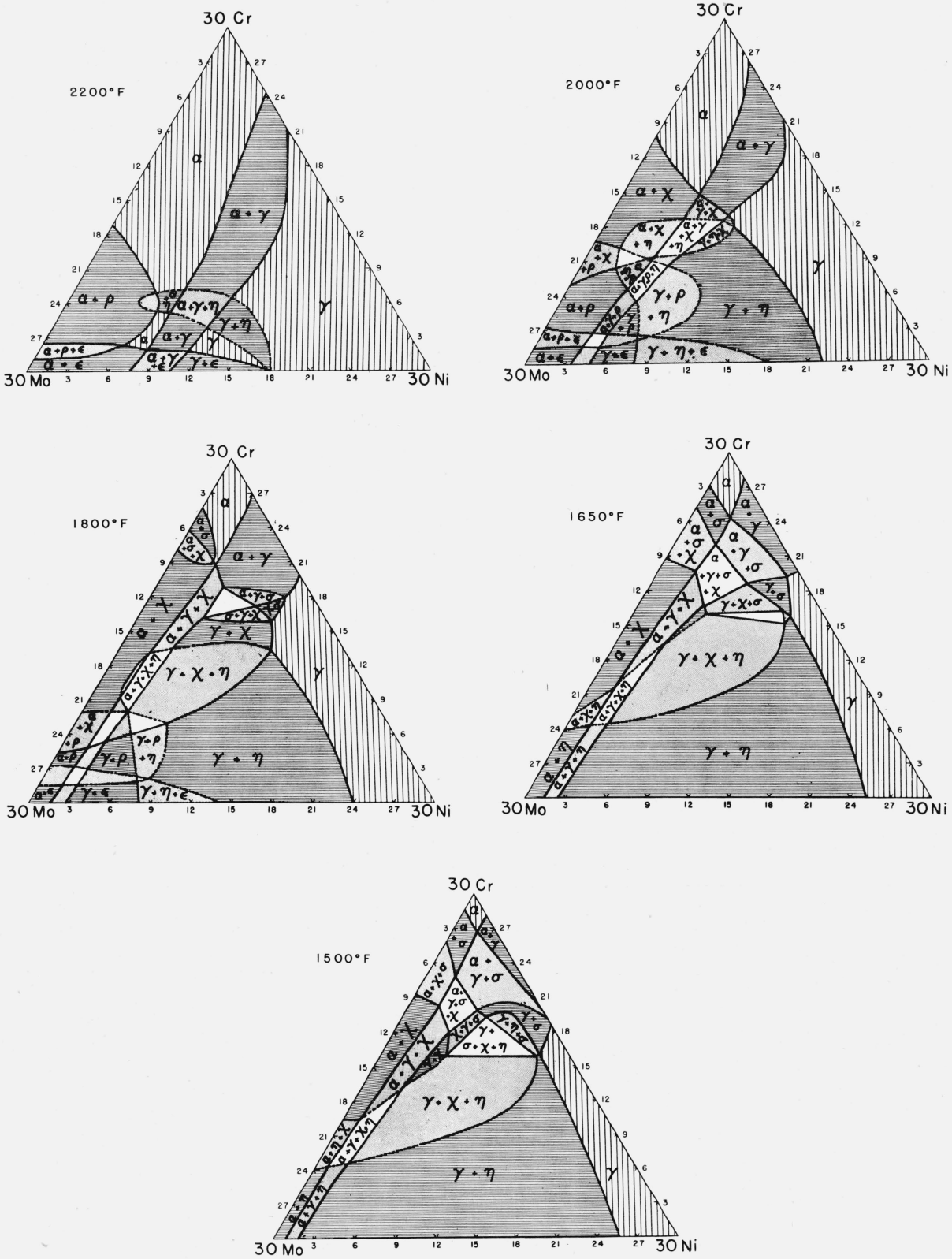

FIGURE 22. *Phase diagrams for iron-chromium-molybdenum-nickel alloys containing 70 percent of iron at 2,200°, 2,000° 1,800°, 1,650°, and 1,500° F.*

5. Summary

Alloys containing 70 and 80 percent of iron, and percentages of chromium, molybdenum, and nickel varying from 0 to 30 and 20, respectively, were prepared from known mixtures of powdered metals, compacted into 2-g pellets, and sintered in dry hydrogen at 2,500° F. Sintered pellets were reheated to 2,200°, 2,000°, 1,800°, 1,650°, and 1,500° F for 25, 75, 250, 500, and 1,000 hr, respectively, and quenched in water. Some pellets were reheated at 2,500° F before reheating at these temperatures. The carbon content of the sintered pellets was less than 0.01 percent, the oxygen content was 0.003 to 0.007 percent, and the nitrogen content was 0.003 percent.

Two soft phases, α Fe and γ Fe, and five hard phases, σ, χ, ϵ, η, and ρ, were identified as stable coexisting phases in the iron-chromium-molybdenum-nickel alloys. The σ, ϵ, and η phases were identified in the iron-molybdenum alloys and have the composition FeMo, Fe_3Mo_2, and Fe_2Mo, respectively. The χ and ρ phases were identified in the chromium-iron-molybdenum alloys. The η and ρ phases have not been identified previously in the iron-molybdenum and chromium-iron-molybdenum alloys, respectively. The composition of ρ in the quaternary alloy containing 70 percent of iron, 4 percent of chromium, 25 percent of molybdenum, and 1 percent of nickel was 53 percent of iron, 4 percent of chromium, and 43 percent of molybdenum. The ρ phase has been identified also in iron-molybdenum-nickel alloys containing 70 percent of iron and in iron-molybdenum alloys, but only in the quenched condition. In this condition the alloys had a characteristic Widmanstäten structure consisting of alternate bands of α Fe and ρ. Diagrams were constructed to show the fields of stability with respect to composition for coexisting phases in the quaternary, ternary, and binary alloys.

The authors are grateful for the assistance of Robert I. Frank, who made many of the residue separations and diffractometer charts that were necessary in the identification of the phases.

6. References

[1] The sigma-phase investigation program of Sub-Committee VI of Committee A–10, Annual Committee Reports, Am. Soc. Testing Materials Proc. **53,** 143 (1953).

[2] H. C. Vacher and C. J. Bechtoldt, Delta ferrite-austenite reactions and formation of carbide, sigma, and chi phases in 18 chromium-8 nickel-3.5 molybdenum steels, J. Research NBS **53,** 67 (1954), RP2517.

[3] W. P. Sykes, Metals Handbook, 1948 ed., p. 1210 (Am. Soc. Metals, Cleveland, Ohio).

[4] G. Bergman and D. P. Shoemaker, The space group of the σ-FeCr crystal structure, J. Chem. Phys. **19,** 515 (1951).

[5] A. J. Cook and F. W. Jones, The brittle constituent of the iron-chromium system (sigma phase), J. Iron Steel Inst. (London) 148, 217 (1943).

[6] J. W. Putnam, R. D. Potter, and N. J. Grant, The ternary system, Cr-Mo-Fe, Trans. Am. Soc. Metals **43,** 824 (1951).

[7] S. R. Baen and P. Duwez, Constitution of Fe-Cr-Mo alloys at 1,200° F, Trans. Am. Inst. Mining Met. Eng. **191,** 331 (1951).

[8] T. Takei and T. Murakami, On the equilibrium diagram of the iron-molybdenum system, Trans. Am. Soc. Steel Treating **16,** 339 (1929).

[9] H. J. Goldschmidt, A molybdenum sigma phase, Research (London) **2,** 343 (1949).

[10] W. P. Sykes, Discussion to reference [7], Trans. Am. Soc. Steel Treating **16,** 358 (1929).

[11] W. K. Andrews, A new intermetallic phase in alloys steels, Nature **164,** 1015 (1949).

[12] J. G. McMullin, S. F. Reiter, and D. G. Ebeling, Equilibrium structures in Fe-Cr-Mo alloys, Trans. Am. Soc. Metals **46,** 799 (1954).

[13] J. S. Kasper, The ordering of atoms in the chi-phase of the iron-chromium-molybdenum system, Acta Metallurgica **2,** 456 (1954).

[14] H. Arnfelt, On the constitution of the iron-tungsten and iron-molybdenum alloys, Iron Steel Inst. (London) Carnegie Schol. Mem. **17,** 1 (1928).

[15] H. Arnfelt and A. Westgren, De intermediara fasernas kristallbyggnad och sammansättning i jära-volfram och järn-molybdenlegeringer, Jernkontorets Ann. **119,** 185 (1935).

[16] W. P. Sykes, The iron-molybdenum system, Trans. Am. Soc. Steel Treating **10,** 839 (1926).

[17] Dilip K. Das and Paul A. Beck, Survey of portions of the iron-nickel-molybdenum and cobalt-iron-molybdenum ternary systems at 1,200° C, Nat. Advisory Comm. Aeronaut. Tech. Note 2896 (1953).

[18] Kehsin Kuo, Discussion to reference [19], Trans. Am. Soc. Metals **47,** 227 (1955).

[19] F. L. VerSnyder and J. J. Beattie, Jr., The Laves and chi phases in a modified 12-chromium stainless alloy, Trans. Am. Soc. Metals **47,** 211 (1955).

[20] R. P. Zaletaeva, H. F. Lashko, M. D. Nesterova, and S. A. Iuganova, A new intermetallic compound in the binary system Fe-Mo, Doklady Akad. Nauk SSSR **81,** 415 (1951).

[21] E. Vigouroux, Sur les ferromolybdenes purs, Compt. rend. **142,** 889 and 928 (1906).

[22] H. J. Goldschmidt, Phase diagrams of the ternary system Fe-Cr-W and Fe-Cr-Mo at low temperatures, Iron Steel Inst. (London) Symposium on high temperature steels for gas turbines, p. 249 (1951).

[23] H. J. Goldschmidt, A further high temperature σ-phase and a note on σ-ξ relations, Research (London) **4,** 343 (1951).

[24] Sheldon Paul Rideout and Paul A. Beck, Survey of Portions of the chromium-cobalt-nickel-molybdenum quaternary system at 1,200° C, Nat. Advisory Comm. Aeronaut. Tech. Note 2683 (1952).

[25] Sheldon Rideout, W. D. Manly, E. L. Kamen, B. S. Lement, and Paul A. Beck, Intermediate phases in ternary alloy system of transition elements, Trans. Am. Inst. Mining Met. Eng. **191,** 872 (1951).

[26] C. S. Barrett, A. H. Geisler, and R. F. Mehl, Mechanism of precipitation from the solid solution of silver in aluminum, Trans. Am. Inst. Mining Met. Eng. **143,** 134 (1941).

[27] W. P. Rees, B. D. Burns, and A. J. Cook, Constitution of iron-nickel-chromium alloys at 650° C to 800° C, J. Iron Steel Inst. (London) **162,** 325 (1949).

[28] P. Schameister and R. Ergang, Das Zustandsschaubild Eisen-Nickel-Chrom unter besonderer Berücksichtingung des nack Dauerglühunger auftretenden spräden Gefügebestandteiles, Arch. Eisenhüttenw. **12,** 459 (1939).

[29] C. H. M. Jenkins, E. H. Bucknall, C. R. Austin, and G. A. Mellor, The constitution of the alloys of nickel, chromium, and iron, J. Iron Steel Inst. (London) **136,** 187 (1937).

WASHINGTON, August 7, 1956.